Microchimica Acta (2021) 188: 381
https://doi.org/10.1007/s00604-021-05031-5

ORIGINAL PAPER

Lateral flow colorimetric biosensor for detection of *Vibrio parahaemolyticus* based on hybridization chain reaction and aptamer

Na Ying[1] · Yuan Wang[1] · Xuefeng Song[1] · Liguo Yang[1] · Bo Qin[1] · Yanqing Wu[1] · Wenhong Fang[1]

Received: 24 June 2021 / Accepted: 17 September 2021 / Published online: 15 October 2021

Abstract

Vibrio parahaemolyticus (*V. parahaemolyticus*) is the causative agent for acute hepatopancreatic necrosis disease (AHPND) of shrimp, and it is also a common seafood-borne pathogen for humans. Rapid and accurate identification of *V. parahaemolyticus* is helpful to diagnose the AHPND and ensure food safety. Common detection methods suffer the deficiency of time-consuming and complexed operation. Based on the increased development of aptamer and our previous study, a new detection assay of *V. parahaemolyticus* was introduced, in which the aptamer combined with magnetic nanoparticles (MNPs) was the recognizer, hybridization chain reaction (HCR) was the signal amplifier, and lateral flow nucleotide biosensor (LFNB) was the signal exporter. The assay possessed high specificity of distinguishing the target with other bacteria, and the calculated limit of detection was 2.6×10^3 cells. Furthermore, the whole process just needs 67 min, free of thermocycle instruments and signal readout instruments, which means it is suitable for low-resource laboratories or districts.

Keywords *Vibrio parahaemolyticus* · Aptamer · Magnetic nanoparticles · Hybridization chain reaction · Lateral flow nucleotide biosensor · Colorimetric detection

Introduction

Vibrio parahaemolyticus is a Gram-negative rod-shaped bacterium that is ubiquitous in nature, and it is the causative agents for acute hepatopancreatic necrosis disease (AHPND) [1], a disease responsible for a 33% drop in cultured shrimp production [2]. *V. parahaemolyticus* is also a kind of common seafood-borne pathogen, and eating improperly processed seafood contaminated with *V. parahaemolyticus* may cause gastroenteritis [3]. When the ingested content of *V. parahaemolyticus* reach 240 MPN/g, it can cause 72% infection rate [4]. Rapid and accurate identification of *V. parahaemolyticus* is not only helpful to ensure food safety but also to diagnose the AHPND, preventing the big economic loss for aquaculture.

In fact, any detection methods of bacteria are nothing but three parts: target recognizing, signal amplification, and signal output; they were the keys and quintessence of the detection methods. Quantitative [5] and nested polymerase chain reaction (PCR) [6]were often used for *V. parahaemolyticus* detection, which target the virulence gene of bacteria, amplify the signal by PCR, and output the signal by the melting curve or electrophoresis. They pose the high sensitivity but suffer the expensive thermal cycling instruments and complicated procedures. In recent years, various signal output biosensors combined with isothermal amplification methods, such as strand displacement amplification (SDA), loop-mediated isothermal amplification (LAMP), and recombinase polymerase amplification (RPA), were developed for pathogen bacteria detection [7–14]. Among these, lateral flow nucleotide biosensors (LFNB) and hybridization chain reaction (HCR) [15] are more focused because the former is friendly operation and point-of-care (POC) and the latter is amplified at room temperature (RT), free of precise thermal cycling instruments and free of enzymes.

In our previous study, a LFNAB combined with HCR for detection of *Salmonella* [16] was introduced. However, this biosensor suffered from the whole tedious detection period because it targeted 16S rRNA, and the RNA extraction process was complex. In this study, an improved biosensor for detection of *V. parahaemolyticus* was introduced. We continued to apply HCR for signal enhancement and the LFNB for signal output because of their advantages of convenience.

✉ Wenhong Fang
fwenhong@163.com

[1] East China Sea Fisheries Research Institute, China Academy of Fishery Sciences, Shanghai 200090, China

Furthermore, the previously screen out aptamer of *V. parahaemolyticus* [17], acting as the target components, was applied. Aptamer is synthetic single-strand oligonucleotide, coming from systematic evolution of ligands by exponential enrichment (SELEX) [18]. It possesses the high affinity to many kinds of target, such as metal iron [19], biological molecular [20, 21], and even the whole cell [17, 22]. Nevertheless, the application of current aptasensors is easy to generate false-positive or strong background signal because the ligand-specific receptor and aptamer-complementary element (ACE) [23] were mixed in the same solution. In this study, for avoiding the generated false-positive results, magnetic nanoparticles(MNPs), containing rapid solution kinetics and high surface volume ratios to ensure magnetic separation of targets [24], were applied to separate the recognizing element from the signal element.

The purpose of this study was to establish a convenient and fast assay for *V. parahaemolyticus* detection by combining LFNB and HCR with aptamer. And we hope the application of this assay may be helpful to food safety control or shrimp aquaculture, especially in low-resource districts.

Materials and methods

Materials and instruments

All bacterial strains were listed as follows: *V. parahaemolyticus* (ATCC 17,802), *V. splendidus* (ATCC 33,869), *V. vulnificus* (ATCC 27,562), *V. alginolyticus* (ATCC 17,749), *Salmonella typhimurium* (ATCC 10,420), *Listeria monocytogenes* (ATCC 19,115), and *Escherichia coli* (ATCC 25,922). The oligonucleotides (listed in Table 1) were synthesized by Sangon Biotech Co., Ltd. (Shanghai, China) and purified using high-performance liquid chromatography. All oligonucleotides were dissolved in sodium phosphate sodium chloride buffer solution (SPSC; 150 mM Na2HPO4, 0.75 M NaCl, pH 7.4) to a storage concentration of 10 mM. Magnetic beads modified with streptavidin (Dynabeads™ M-280 Streptavidin, 2.8 μm, 10 $mg{\cdot}mL^{-1}$) were purchased from Invitrogen (Carlsbad, CA, USA). Colloidal AuNPs (0.01%, 20 nm) were purchased from Hualan Chemical Co., Ltd. (Shanghai, China). Streptavidin (SA, 18 μg/mL) was also purchased from Sangon Biotech. Nitrocellulose (NC) filter membrane was purchased from Millipore (Billerica, MA, USA, www.merckmillipore.com). Absorbent pad, sample pad, and conjugate pad were purchased from Nanjing Microdetection Biotechnology Co., Ltd. (Nanjing China, www.microdetection.cn). BSA-biotin conjugates was purchased from Xi'an Kaixin Biological Technology Co., Ltd. (Xi'an, China).

High speed centrifuge (Model: TG16-WS) was purchased from Hunan Xiang Yi Laboratory Instrument Development Co., Ltd. (Changsha, China, www.cence.cn); Biodot AD3200 Dot Dispensing system (BioJet), AirJet HGS102, and Biodot CM4000 strip cutting machine were obtained from BioDot Inc. (California, USA, www.biodot.com); ultraviolet spectrophotometer was obtained from Shanghai Xianke Spectroscopic Instrument Co., Ltd. (Shanghai, China).

Table1 Sequences used in this study

Probe name	Abbreviation	Sequence (5′-3′)	Sequence length (nt)
Hairpin1-biotin	H1-bio	Biotin-TTTTTTTTAACCCACGCCGAATCCTAGACTCAAAGTAGTCTAGGATTCGGCGTG	54
Hairpin1-biotin	H1-bio	TTTTTTTTAACCCACGCCGAATCCTAGACTCAAAGTAGTCTAGGATTCGGCGTG-Biotin	54
Initiator probe	IP	ATTAGTCAAGAGGTAGACGCACATA**AGTATCTCAA**AGTCTAGGATTCGGCGTGGGTTAA	59
Aptamer of *V. parahaemolyticus*	A3P	ATAGGAGTCACGACGACCAGAATCTAAAAATGGGCAAAGAAACAGTGACTCGTTGAGATACTTATGTGCGTCTACCTCTTGACTAAT	87
Forward primer of A3P	FP	ATAGGAGTCACGACGACCAGAA	22
Reverse primer of A3P	RP	ATTAGTCAAGAGGTAGACGCACATA	25
Capture probe1	CP-1	TTTCTTTGCCCATTTTTAGATTCTGGTCGTCGTGACTCCTAT	42
Capture probe2	CP-2	TCTTTGCCCATTTTTAGATTCTGGTCGTCGTGACTCCTAT	40
Capture probe3	CP-3	TTTGCCCATTTTTAGATTCTGGTCGTCGTGACTCCTAT	38
Capture probe4	CP-4	TTTGCCCATTTTTAGATTCTGGTCGTCGTGACTCCTA	37

*In initiator probe and capture probes, complementary sequences of aptamer were underlined

Preparation of LFNB

LFNB was designed, prepared, and assembled as described previously [16], with some modifications. Briefly, 0.01% colloidal gold particles (AuNPs) were obtained by reduction of gold chloride (20nm) with 1% sodium citrate. K2CO3 solution (0.1 mol/L) was added in colloidal AuNPs to adjust pH to 8.0 before SA was added to AuNPs at a final concentration of 18 μg mL^{-1} to form AuNPs-SA. This mixture, dispensed by Biodot AD3200 with AirJet, was impregnated on the conjugate pad of the biosensor. Test line (T line) and control line (C line) were all dispensed by Biodot AD3200 with BioJet. The capture probe, with the final concentration of 10 nM, was coated on the surface of a NC filter membrane at 1 μL/cm as the T line, and BSA-biotin conjugate (1.2 mg mL^{-1}) was coated on the surface of the NC membrane at 1 μL/cm as the C line. The LFNB was assembled with the absorbent pad, the NC membrane (in the middle), and absorbent pad and was then cut into 0.5-cm-wide, 5-cm-long pieces dipstick by Biodot CM4000. All the strips were sealed in a plastic bag and stored until used (refrigeration, from light, valid for 12 months).

Hybridization chain reaction

Hairpin probes, beacon structure with sticky end, were designed referred to the previous study [15] with some modification, and the design principle was based on the combination of criteria: sequence symmetry minimization [25], the probability of adopting the target secondary structure at equilibrium [26], the average number of incorrect nucleotides at equilibrium relative to the target structure [27], and hybridization kinetics [28]. H1-Bio and H2-Bio were diluted to 10μM by SPSC buffer, and initiator probe was diluted to 3μM. Hairpin probes were heated to 95°C for 5 min and then cooled to room temperature for 1 h before the equal volume mixing of H1-Bio, H2-Bio, and IP and standing at RT for 2 h at least. The prepared HCR products can be stored at 25°C at least for 3 months.

Recognition of V. parahaemolyticus by aptamer and separation by magnetic beads

The bacteria were cultured in Luria-Bertani (NaCl 20‰) liquid medium, and the concentration was calculated by the standard curve of optical density, measured by ultraviolet spectrophotometer. The bacteria (10^4~10^{10}cells) were first gathered by centrifugation (13,000rpm, 2min), washed with phosphate buffered solution (PBS) for 3 times (5 min), and then incubated with biotin modified aptamer—A3P (2 nmol) in thermostatic shakers (37°C, 100rpm, 30min). After centrifugated the mixture, the unbound aptamer in the supernatant was discarded, and PBS was added to resuspend the sediment. The procedure of centrifugation, removal of supernatant, and resuspension was repeated for 3 times (5min). To enrich the target bacteria, 50μL coated magnetic bead (SA-MB, 200μg/mL) solutions was added to the sediment and incubated in thermostatic shakers (37 °C, 100rpm, 5min). After magnetic separation with magnet, the non-target cells and impurities in the supernatant were removed, and 3 times of washing by PBST (PBS supplemented with 0.05% Tween-20) was performed (5 min). The acquired complex sediment was used for the following steps.

Verification of aptamer separation performance

PCR was performed to verify the above separation performance; 1μL forward and reverse primers of A3P, 12.5μL Taq PCR master mix, and 10.5μL ddH_2O were added to the enriched sediment to perform the PCR. The amplification of aptamer (A3P) procedure was as follows: 20 cycles of denaturation at 94 °C for 30 s, annealing at 55 °C for 30 s, and extension at 72 °C for 30 s; then the amplified product was applied in 9% native polypropylene acyl amine gel electrophoresis (PAGE).

Visual detection of V. parahaemolyticus by aptamer-HCR-LFB

For visual detection, HCR products (10μL), prepared in advance, were added to the enriched complex, got from Section 2.4, and incubated at 25°C for 15min. The mixture (10μL) and running buffer (20μL, 25% saline sodium citrate buffer containing 4% BSA) were subsequently added on sample pad of LFNB prepared. As the solution migrated up by capillary force, the red line of test zone appeared if the aptamer was existing with enough quantity (5min). Then, the result of the test lines (peak areas) was scanned by HP scanner (HP LaserJet Pro MFP M226dn).

Real sample assay to detection of V. parahaemolyticus by aptamer-HCR-LFNB

To assess the dependability of the assay, recovery experiments were performed by shrimp sample. Twenty grams of fresh shrimp was aseptically (boiling sterilization) added to 200 mL saline solution (20‰) and then was homogenized for 2 min (m/v = 10%). One milliliter was respectively taken and mixed with bacteria sediments, separately containing 10^4, 10^6, and 10^8 cells (measured by ultraviolet spectrophotometer), to make samples under detection. The following steps, including centrifugation, washing with PBS, incubating with aptamer, separation by MBs, and visual detection by LFNB, were the same with the procedures in Sects. 2.4 and 2.6. Meanwhile, the amount of bacteria was also measured by the plate counting method. The recovery (%) was calculated by (the detection

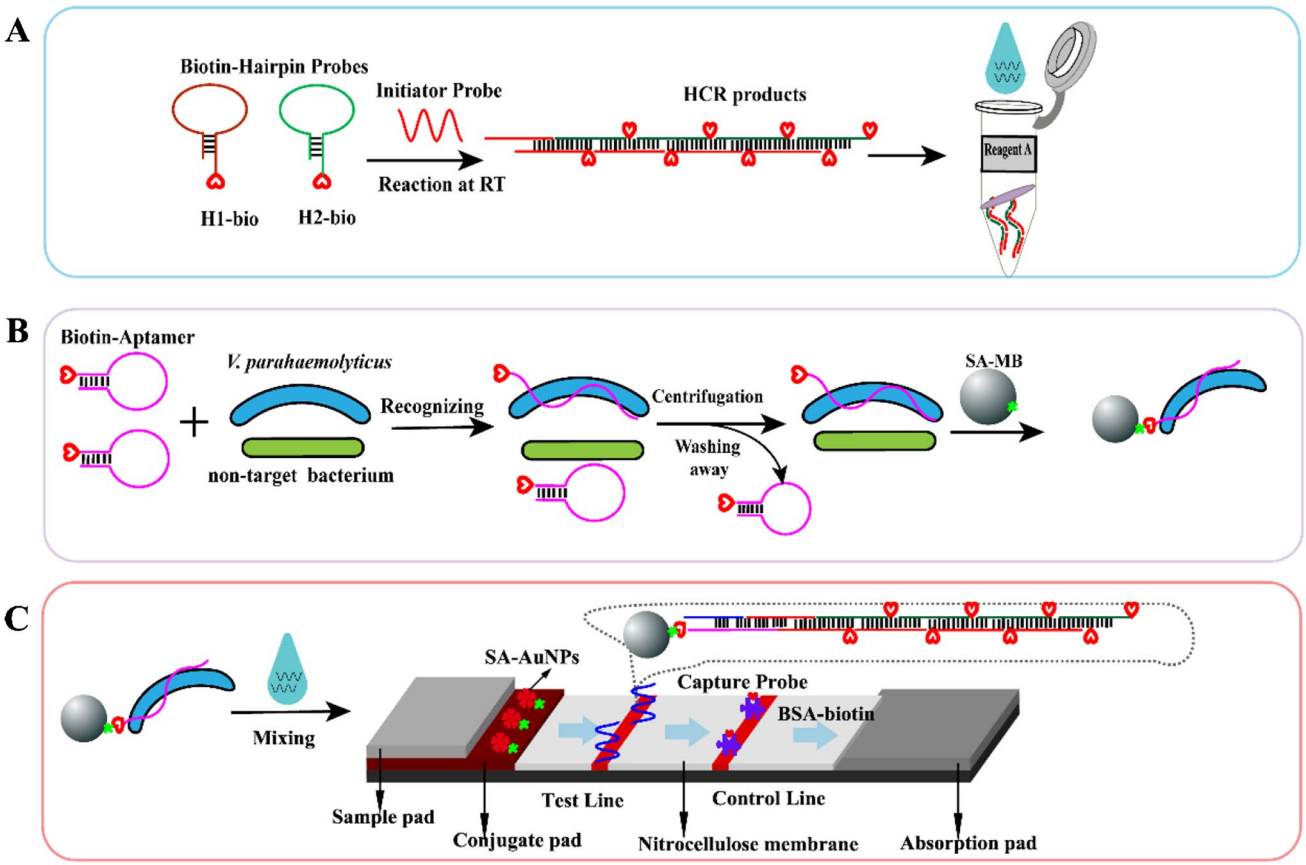

Scheme 1. Schematic illustration of aptamer-HCR-LFNB. **A** HCR products were prepared. **B** Recognition of *V. parahaemolyticus* by aptamer and separation by magnetic beads. **C** Visual detection of V. *parahaemolyticus* by aptamer-HCR-LFNB

value by this assay)/(the detected bacteria by traditional plate counting method) ($n = 6$).

Statistical analysis

For quantitative analysis, the scanned image was treated by ImageJ software [29]. It was first switched to grayscale (Image-Type-8 bit), then rectangularly selected the test lines and control lines, and numbered them. When the rectangular selection number reached to 3, the peak plots were automatically appeared. Then peak area was measured (Analyze-Measure), acting as quantitative data and analyzed in the following steps. All data in this study was acquired by three repeated experiments. The mean value and standard deviation of T/C peak area ratio were calculated by Origin 9 software, and linear analysis was also performed by it (Analysis-Fitting-Linear Fit).

Results and discussion

Principle of aptamer-HCR-LFB assay

The principle was illustrated in Scheme 1. As shown in Scheme 1A, two hairpin probes with potential energy maintained a sub-steady state at RT. When the initiator probe (IP), composed of trigger sequence of HCR and matching sequence of aptamer, was added to the hairpin mixture, it first hybridized with the sticky end of H1-bio, gradually opened the hairpin structure through strand replacement reaction, and simultaneously released the initiator sequence for H2-bio. After the chain reaction between H1-bio and H2-bio, a long double-helix polymer-labeled biotin was formed, stored as reagent A. For

recognizing and separation of target cell (Scheme 1B), aptamers were first added in the sample. The target cell was recognized by the aptamer, and the complex was subsided after the centrifugation, and the supernatant containing residual and unbound aptamer was discarded. After the addition of magnetic beads, the non-target cell in the supernatant, free of aptamer-biotin-SA-MB, was removed. For visual detection (Scheme 1C), the complex of aptamer-biotin-SA-MBs was mixed with HCR products, and the matching sequence of IP banished the bacteria from aptamer due to the longer complementary sequence and combined with aptamer more powerfully. When the mixture was applied on sample pad, it slowly migrated to conjugated pad, and streptavidin-coated AuNPs were conjugated to the tagged HCR products of the complex by the biotin-streptavidin linkage. When it reached the test line, the part of aptamer matched with capture probe (CP). Subsequently, the complex was captured by CP immobilized on test line (TL), and the accumulation of AuNPs was visualized as a characteristic red band. The excess SA-AuNP conjugates continued to move and were captured on the control line (CL) by reactions between biotin and SA on the AuNP surface, thus forming a second red band. However, the red band of test zone would not appear in the absence of target bacteria.

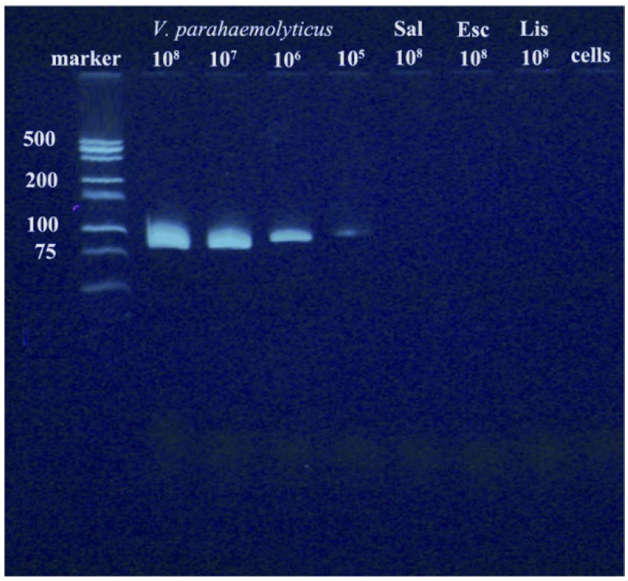

Fig. 1 Separation effect of target and non-target bacteria by aptamer and magnetic beads. All the PCR products were applied by 9% native PAGE with voltage of 140v (20 min). The concentration of *V. parahaemolyticus* was 10^8–10^5 CFU mL^{-1}; and the non-target bacteria were 10^8 CFU mL^{-1}

The verification of aptamer separation effect

The aptamer sediments (Sect. 2.4), isolated from different concentrations of *Vibrio parahaemolyticus* and control groups, *Salmonella enteritidis* (Sal), *Escherichia coli* (Esc), and *Listeria monocytogenes* (Lis), were applied in PCR test, and electrophoresis was used to verify the effect. As shown in Fig. 1, the target fragment (87 bp) was not amplified in the non-target bacterial sediment. The 10^5 cell of *V. parahaemolyticus* just appeared a weak band, and the band gradually brightened with increase of the bacterial concentration, which also means that the content of aptamer in the isolated complex is proportional to the target bacteria. We consider that the separation process of aptamer from target bacteria is effective and this also means the following experiment is feasible.

The efficiency and stability of HCR product

At present, most of the signal amplification methods used for detection are based on the target, such as LAMP and PCR. That is, the amplification program cannot be started before the target is separated, which also limits the detection period. In this assay, HCR can be initiated and prepared in advance, as a reagent, and this may reduce the detection time. But the efficiency of signal amplifier and its validity period should be known. Native gel electrophoresis of HCR product is shown in Fig. 2, and the resulting polymers and

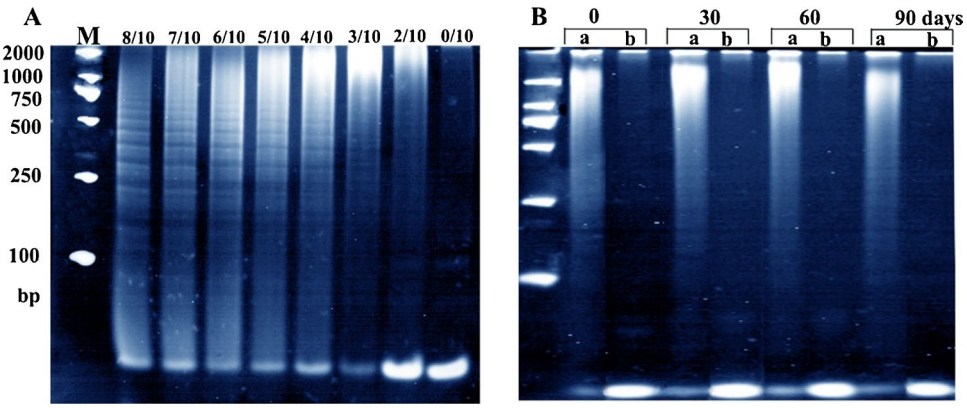

Fig. 2 **A** The HCR efficiency effected by the ration of IP/hairpin probes. **B** The stability of HCR products with storage time of 0 day, 30 days, 60 days, and 90 days. Notes: a, HCR products stored at RT; b, HCR in the absence of IP

residual probes revealed the efficiency and stability of HCR. As shown in Fig. 2a, the efficiency varied with the ratio of IP/hairpin probes: On the ration of 3/10, the products get the maximal molecular and the highest efficiency. The higher ratios revealed the smaller and heterogeneous polymers, which may be interpreted as competition effect. At the beginning, the hairpin probes were adequate, and the long polymers were formed, but as the reaction time went on, the reactants were in short, and the accumulation had to be decelerated or aborted, resulting in the shorter and inhomogeneous polymers. On the contrary, less trigger sequences were easy to get polymers of higher molecular weight. But the accumulation requires time, which means the limited polymers were generated and mass probes were remained within a certain period. However, there is no obvious difference between the newly acquired products and products stored for 30, 60, and 90 days at RT (Fig. 2b). In another word, the HCR product can be stored stably at least for 3 months, which also provided the possibility for the production of commercial detection kit.

The right sequence of capture probe

The CP and IP were designed based on aptamer, and they are separately complementary to part of aptamer. However, the used aptamer has part of self-complementary sequence, likely hairpin structure, which means inappropriate design of CP and IP will cause complementary with each other in the absence of target. Thus, the optimization of CP sequence was required to avoid the false complementary, and the result is shown in Fig. 3A; redline was seen on CP1 (42nt), CP2 (40nt), and CP3 (38nt) in the absence of target cell, but no line of CP4 (37nt). As the length of mismatched sequence was shorten, the strength of false-positive line was weakened (CP-1 > CP-2 > CP-3). When the CP-4 was used, the red line of false positive disappeared, meaning the CP-4 sequence is not complementary with IP any more. The shorter sequence (< 37nt) will also result the good specificity, but the longer complementary sequence means the more stability of aptamer/CP. Therefore, CP-4 (37nt) was the right sequence.

Selectivity and detectability of aptamer-HCR-LFNB

Specificity is the criteria of the detection method. In this assay, the separation of aptamers from the sample is the key step to the specificity, and it has been verified by electrophoresis in the above section. Here, we verify the specificity again by the test strip. As shown in the Fig. 4A, only the target group is positive, and the results of non-target strains, *V. splendidus*, *V. vulnificus*, *V. alginolyticus*, *Salmonella enteritidis*, *Escherichia coli*, and *Listeria monocytogenes*, were all negative on the test strip, which means the whole-cell aptamer was specific for recognizing the target. In addition, we also explored the detectability of the method, seen as Fig. 4B–D. When the *V. parahaemolyticus* is 10^4 cells or over, the positive results can be detected, and the brightness of the TL strengthened with the increase of the target. When the *V. parahaemolyticus* is 10^3 cells, the red line was weak and sporadic. A linear relationship was also observed between peak area ratio and the target cell density logarithmic scale, in the range 10^3–10^8 CFU mL^{-1}. A correlation coefficient of 0.98 (Fig. 4D) was also recorded and the linear equation was $Y = 21.42X - 64.80$. The calculated LOD was 2.6×10^3 cells, according to 3σ/slope of the calibration curve, and the σ is the standard deviation of the blank sample ($n = 20$).

As we know, the LOD of diagnostic methods depends on the amount of recognizable target, the efficiency of signal amplification, and sensitivity of signal readout ways. For example, targeting the multi-copy 16S rRNA,

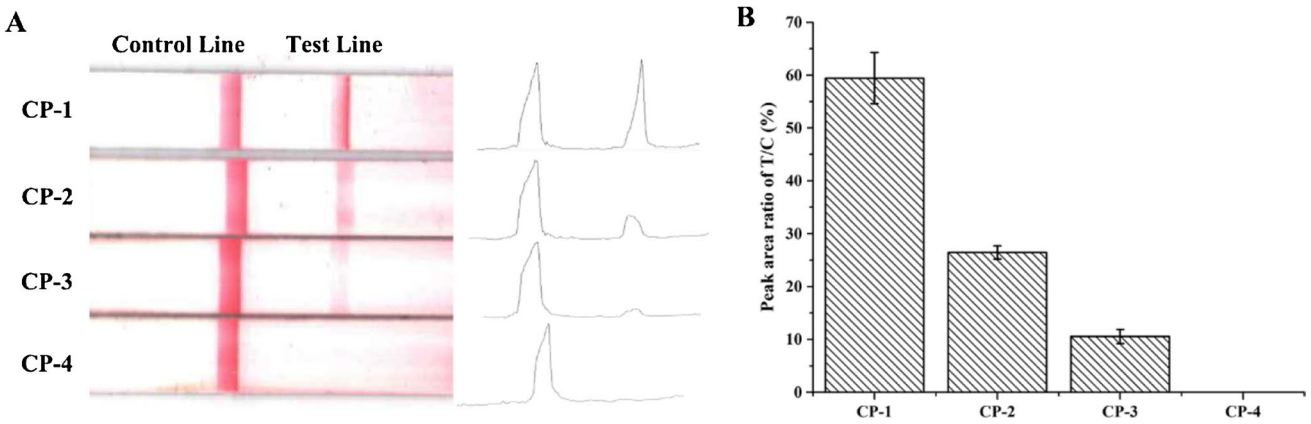

Fig. 3 The optimization of the capture probe. **A** Photographic images of detection performance by different capture sequences in the absence of aptamer. "CP-1" representing capture probe1 was coated in test line, and similarly with CP-2, CP-3, and CP-4 in the same concentration. **B** The corresponding optical responses of images

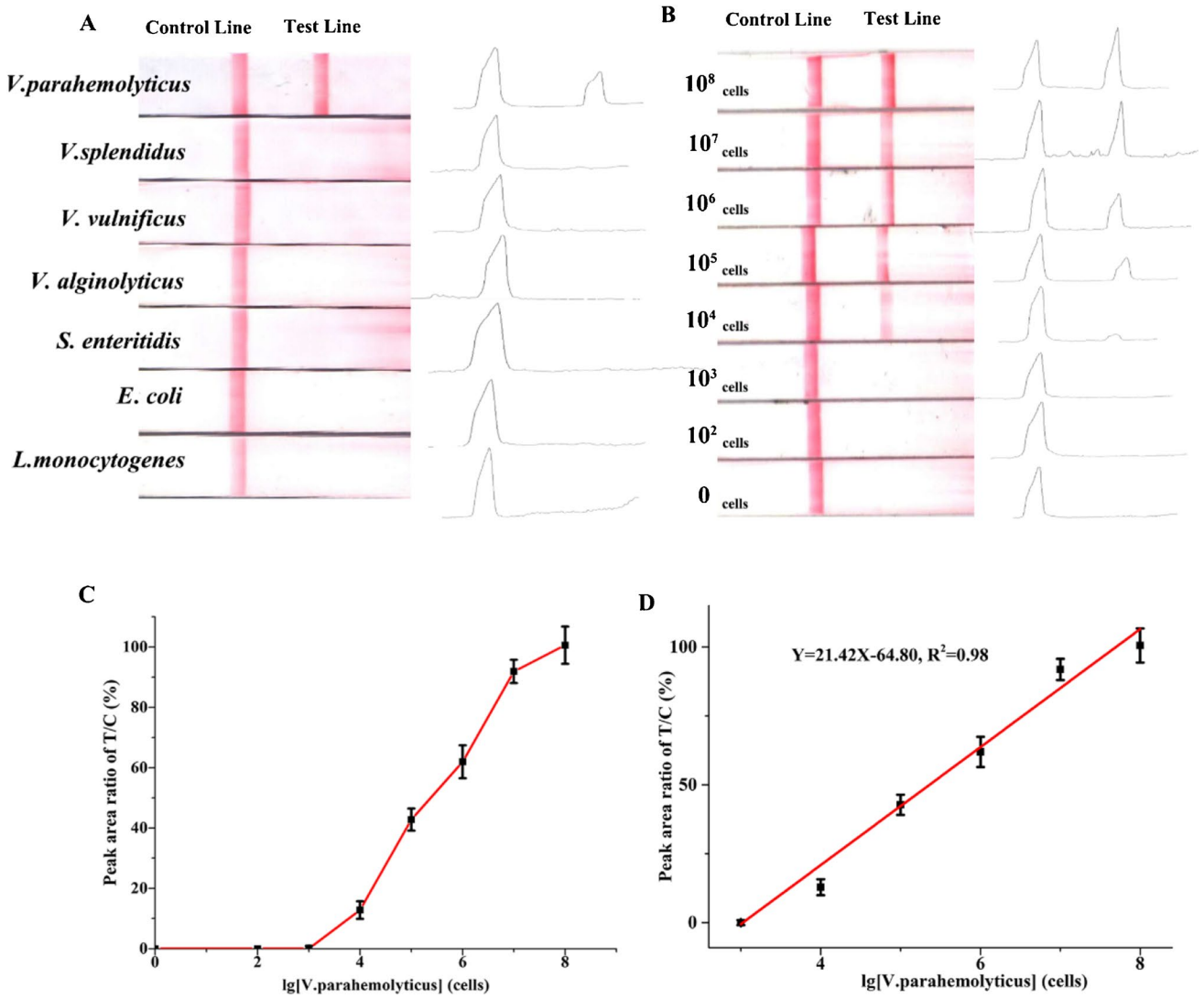

Fig. 4 Selectivity (**A**) and sensitivity (**B**) of aptamer-HCR-LFNB. The representative bacteria in selective experiment were as follows: *V. parahaemolyticus*, *V. splendidus*, *V. vulnificus*, *V. alginolyticus*, *Salmonella enteritidis* (*S. enteritidis*), *Escherichia coli* (E. *coli*), and *Listeria monocytogenes* (L. *monocytogenes*). All bacteria were used at a cell density of 10^8 CFU mL^{-1}. **C** Calibration curve of the detection of *V. parahaemolyticus* by aptamer-HCR-LFNB. Y is the peak area ratio of T line/C line, and X is logarithmic of *V. parahaemolyticus* concentrations from 10^2–10^8 CFU/mL. **D** Linear relationship between the peak area rations and logarithmic of *V. parahaemolyticus* concentrations from 10^4 to 10^8 CFU/mL. All the values were calculated by three measurements

compared to targeting the whole cell, will get the lower detection limit. And if the resulted signal was fluorescence, electrochemical signal, etc., the recognition will be more sensitive. This method targeted the whole cell, meaning that the recognizable cells were equal or less than (may interfered by some factors) the real existing cell in the sample. Importantly, the amplification magnitude of HCR was about 2–3 orders [16, 30], lower than 10^9-fold of loop-mediated isothermal amplification (LAMP) in 1 h [31], 10^5-fold of strand displacement amplification (SDA) in 30 min [32], 10^9-fold of nucleic acid sequence-based amplification (NASBA) [33], 10^7-fold of recombinase polymerase amplification (RPA) [34], etc. All of above may account for the high LOD of this assay, compared with other bacteria detection methods (Table S1). However, the biosensor was originally positioned to point-of-care products, avoiding the precise instruments, suitable for non-laboratory places and requiring the shortest detection period, and furthermore, the LOD of this assay is sufficient for food safety detection and disease diagnosis.

In addition, the reproducibility of this assay was identified by detection of *V. parahaemolyticus* at quantity of 10^4 cells, 10^5 cells, and 10^6 cells. The coefficients of variation (CV, Sd/mean × 100%), respectively was 2.19%, 2.27%, and 2.43% (in quintuplicate), which indicated the acceptable reproducibility of the aptamer-HCR-LFNB.

Detection of V. parahaemolyticus in real sample by aptamer-HCR-LFNB

The recovery (%) of *V. parahaemolyticus* from the real samples was is in Table S2. According to the data, this method showed an acceptable capacity of resisting disturbance, with the recovery ranging from 97.1 to 107.9% and a relative standard deviation (RSD) of 1.9–9.8% ($n = 6$). These results also demonstrated that the aptamer-HCR-LFNB possessed the capabilities for *V. parahaemolyticus* detection from real sample.

Conclusion

Fast and convenient detection methods for *V. parahaemolyticus* are desiderated because it is a threat to food safety and shrimp culture. In this study, the aptamer-HCR-LFNB for the detection of *V. parahaemolyticus* was proposed. Whole-cell aptamer combined with MNPs for recognizing the target, ensured the specificity; HCR, prepared in advance, saved the period detection; and LFNB for signal exporting, avoided the application of equipment. The combination of these components guaranteed the convenience and the accuracy. And we hope this operation-friendly and short time-consuming biosensor can be used in detection of *V. parahaemolyticus*, especially in low-resource districts.

Supplementary Information The online version contains supplementary material available at https://doi.org/10.1007/s00604-021-05031-5.

Acknowledgements We gratefully acknowledge the support from Central Public-interest Scientific Institution Basal Research Fund, CAFS (No. 2020TD41), and Agriculture Research System of Shanghai, China (Grant No. 201405).

References

1. Tran L et al (2013) Determination of the infectious nature of the agent of acute hepatopancreatic necrosis syndrome affecting penaeid shrimp. Dis Aquat Org 105(1):45–55
2. Fisheries DO (2013) Available from: https://www.fisheries.go.th/ems/. Accessed 16 May 2013.
3. Yeung P, Boor K (2004) Epidemiology, pathogenesis, and prevention of foodborne Vibrio parahaemolyticus infections. Food Pathogens Dis 1(2):74–88
4. Hara-Kudo Y, Takatori K (2011) Contamination level and ingestion dose of foodborne pathogens associated with infections. Epidemiol Infect 139(10):1505–1510
5. Han JE et al (2015) qPCR assay for detecting and quantifying a virulence plasmid in acute hepatopancreatic necrosis disease (AHPND) due to pathogenic Vibrio parahaemolyticus. Aquaculture 442:12–15
6. Dangtip S et al (2015) AP4 method for two-tube nested PCR detection of AHPND isolates of Vibrio parahaemolyticus. Aquacult Rep 2:158–162
7. Sun Y et al (2019) Colorimetric aptasensor based on truncated aptamer and trivalent DNAzyme for Vibrio parahemolyticus determination. J Agric Food Chem 67(8):2313–2320
8. S B, et al (2018) A pregnancy test strip for detection of pathogenic bacteria by using concanavalin A-human chorionic gonadotropin-Cu(PO) hybrid nanoflowers, magnetic separation, and smartphone readout. Mikrochimica Acta 185(10): 464
9. Natarajan A et al (2017) An elegant analysis of white spot syndrome virus using a graphene oxide/methylene blue based electrochemical immunosensor platform. Sci Rep 7(1):46169
10. Sha Y et al (2016) A label-free multi-functionalized graphene oxide based electrochemiluminscence immunosensor for ultrasensitive and rapid detection of Vibrio parahaemolyticus in seawater and seafood. Talanta 147:220–225
11. Huang H et al (2016) Label-free 3D Ag nanoflower-based electrochemical immunosensor for the detection of Escherichia coli O157:H7 pathogens. Nanoscale Res Lett 11(1):507
12. Wang W et al (2017) Identification and quantification of eight Listeria monocytogene serotypes from Listeria spp. using a gold nanoparticle-based lateral flow assay. Microchimica Acta 184(3):715–724
13. Xiaohan Y et al (2020) An improved recombinase polymerase amplification assay for visual detection of Vibrio parahaemolyticus with lateral flow strips. J Food Sci 85(6)
14. Jiang W et al (2020) Recombinase polymerase amplification-lateral flow (RPA-LF) assay combined with immunomagnetic separation for rapid visual detection of Vibrio parahaemolyticus in raw oysters. Analyt Bioanalyt Chem 412(7)
15. Dirks RM, Pierce NA, Mayo SL (2004) Triggered amplification by hybridization chain reaction. Proc Natl Acad Sci USA 101(43):4
16. Ying N et al (2017) Visual detection of nucleic acids based on lateral flow biosensor and hybridization chain reaction amplification. Talanta 164:432–438
17. Duan N et al (2012) Selection and identification of a DNA aptamer targeted to Vibrio parahemolyticus. J Agric Food Chem 60(16):4034–4038
18. Tuerk C, Gold L (1990) Systematic evolution of ligands by exponential enrichment: RNA ligands to bacteriophage T4 DNA polymerase. Science 249(4968):505
19. Tan L et al (2017) Colorimetric detection of Hg based on the growth of aptamer-coated AuNPs: the effect of prolonging aptamer strands. Small (Weinheim an der Bergstrasse, Germany) 13(14)
20. Wu D et al (2016) Colorimetric detection of proteins based on target-induced activation of aptazyme. Anal Chim Acta 942:68–73
21. Takahashi M (2018) Aptamers targeting cell surface proteins. Biochimie 145:63–72
22. Majdinasab M, Hayat A, Marty JL (2018) Aptamer-based assays and aptasensors for detection of pathogenic bacteria in food samples. TrAC, Trends Anal Chem 107:60–77
23. JD M, N A, J D (2019) Duplexed aptamers: history, design, theory, and application to biosensing. Chem Soc Rev 48(5): 1390–1419
24. El-Boubbou K, Gruden C, Huang X (2007) Magnetic glyconanoparticles: a unique tool for rapid pathogen detection, decontamination, and strain differentiation. J Am Chem Soc 129(44):13392–13393
25. Seeman NC (1982) Nucleic acid junctions and lattices. J Theor Biol 99(2):237–247
26. Hofacker IL et al (1994) Fast folding and comparison of RNA secondary structures. Monatshefte für Chemie / Chemical Monthly 125(2):167–188
27. Dirks RM et al (2004) Paradigms for computational nucleic acid design. Nucleic Acids Res 32(4):1392–1403

28. Rachofsky EL, Osman R, Ross JBA (2001) Probing structure and dynamics of DNA with 2-aminopurine: effects of local environment on fluorescence. Biochemistry 40(4):946–956
29. Schneider CA, Rasband WS, Eliceiri KW (2012) NIH image to ImageJ: 25 years of image analysis. Nat Methods Tech Life Sci Chem 9(7)
30. Ren W et al (2013) A cytometric bead assay for sensitive DNA detection based on enzyme-free signal amplification of hybridization chain reaction. Biosens Bioelectron 49:380–386
31. Bodulev OL, Sakharov IY (2020) Isothermal nucleic acid amplification techniques and their use in bioanalysis. Biochemistry 85(2)
32. J TB et al (2015) Isothermal strand displacement amplification (iSDA): a rapid and sensitive method of nucleic acid amplification for point-of-care diagnosis. The Analyst 140(22)
33. Compton J (1991) Nucleic acid sequence-based amplification. Nature 350(6313):91–92
34. Lobato I, O'Sullivan C (2018) Recombinase polymerase amplification: basics, applications and recent advances. Trends Analyt Chem : TRAC 98:19–35